# Design and Modeling of an Axial Flux Permanent Magnet Consequent Pole Machine

Mahmoud Marousi Noushabadi [1], Saeid Javadi [*2] & Samad Taghipour Boroujeni [3]

[1] Department of Electrical and Computer Engineering, Kashan Branch, Islamic Azad University, Kashan, Iran

[2] Department of Electrical and Computer Engineering, Kashan Branch, Islamic Azad University, Kashan, Iran

[3] Engeeniering and Technology Department, Shahrekord University, Shahrekord, Iran

## Abstract

Using a consequent pole structure has been common in radial flux machines, and no axial flux machine with a consequent pole structure has been produced so far. This article aims to design an example of an axial flux generator with a simple structure that will reduce magnet consumption, cogging torque, and manufacturing cost without changing the nominal specifications. The proposed generator has a double-sided structure with a sector coil and poles. N identical poles (with only N sequence and iron poles between them) are installed on the rotor and the stator is placed between the rotors. The stator consists of coils that are wrapped concentrically around the teeth. The three-dimensional finite-element numerical methods have been used to evaluate the proposed generator's characteristics. The simulation results of the proposed generator show that the intended goals have been well achieved.

**Keywords: An Axial Flux Machine, Permanent Magnet, Consequent pole, Iron, Generator, Cogging Torque**

## 1-Introduction

Due to the reduction of fossil fuel resources, the trend towards new energies to reduce greenhouse gases, the advancement of battery technology, and the management of the power grid, there has been a fundamental change in the production of electric vehicles [1]. It is expected that the number of customers for these cars will increase rapidly in the future [2]. One of the most important parts of electric cars is the part that converts electric energy to be used in different parts of the car. In modern cars, the amount of electrical energy consumption has increased significantly compared to conventional and old cars [3]. This increase helps to provide more comfort, well-being, and safety for passengers [3]. With the increase in energy consumption, solutions should also be provided to raise the production of electrical energy in these cars. Due to the dimensional limitations of the car engine cabin, the use of generators with high power, high efficiency, small dimensions, and light weight along with a reasonable price (compared to old generators) is one of the important challenges of designers [4]. Meanwhile, axial flux permanent magnet machines are a suitable option for this purpose due to their characteristics such as compact structure, short axial length, lightweight, large power/torque density, low losses, high efficiency, the ability to integrate quickly and easily with other mechanical equipment and the possibility of increasing the number of poles [5, 6]. The appearance of rare-earth permanent magnets such as Nd-Fe-B has created a revolution in the design and construction of axial flux permanent magnet machines in a way that has made it possible to build machines with a large air gap [7]. This development makes it possible for axial flux machines to return to the field of competition [8]. This type of magnet (permanent rare-earth magnets) has a favorable property in terms of residual magnetism density (Br) [9]. In recent years variety range of permanent magnets with a residual flux density (Br) in the range of 1.10-1.49 (T) and the ability to work at a maximum temperature of 80-220 (C°) produced.

Depending on the type of placement of PM in the machine, there are different structures, such as poles mounted on the surface or SPM, consequent poles, internal poles, and poles buried in the rotor [7, 10]. In addition, in other types of PM machines such as flux-switching and flux reverse, the PMs are placed in the stationary part of the machine. Due to the simple structure of SPM and CPPM machines, their use is more common than other types of PM machines [11]. The use of these magnets makes it possible to achieve high power density in a small volume and also helps designers to produce machines with high efficiency and low losses with less material consumption [4, 11]. In recent years, using printed circuit board (PCB) technology, compact axial flux machines with short axial lengths and favorable specifications have been produced. PCB technology can be an attractive alternative to traditional coil winding for the armature of AFPMs [12]. The use of multilayer PCB architecture has proven successful in producing micromotors. The key advantages of using PCB stators in AFPM are ease of manufacturing and maintenance, reduced manufacturing cost, reduced machine components, and their ability to achieve low torque ripple [10, 12]. On the other hand, the biggest drawback of small-slotted PCB motors is their high level of cogging torque, which can prevent the motor from starting in different situations [12]. The shortage crisis of rare-earth permanent magnets and their environmental consequences have directly affected the permanent magnet machine industry, and it seems that the high price and continuous supply of permanent magnets are the biggest threats to this industry.

The desire to reduce the use of rare earth permanent magnets due to their environmental hazards on the one hand and maintaining the characteristics of the machine, on the other hand, has led manufacturers to use new magnetic materials such as a "combination of hard ferrite magnets and soft magnetic composites" or "ferrite permanent magnets" to turn [13,14]. A feasible option to consider is manufacturing an AFPM core using a soft magnetic composite (SMC). SMCs are composed of metal powder coated with an electrically insulating layer and offer several advantages, such as high magnetic flux densities, ease of manufacturing for AFPM cores, and reduced eddy losses due to their high electrical resistivity [7]. However, it should be noted that SMCs are substantially more expensive than steel sheets, and their use is most beneficial when employing strong magnets and high torque densities in the design. It is common to use ferrite core in machines made with PCB technology. The use of a ferrite core and a high number of pole pairs further enhances the motor's efficiency and torque density [10, 12].

Reference [15] has increased the power and torque density by using a Halbach PM array in the rotor of a coreless AFPM. This machine has a double rotor structure and a single PCB stator. Compared to a surface PM topology of the same mass and volume, employing a Halbach array increases torque density by as much as 30% through increased air gap flux density. To increase power and torque density, a combined Halbach array for the axial flux permanent magnet machines (AFPMMs) with a yokeless and segmented armature (YASA) is presented in Reference [16]. The results show that the combined Halbach array with unequal thickness magnets can reduce the amount of permanent magnet material, thus improving the utilization of magnets and reducing costs.

To tackle these problems, reference [17] suggests the use of consequent pole structures for PM machines, which will reduce the consumption of magnets. If the N poles are kept in a machine and ferromagnetic materials such as iron are used instead of the S poles, it leads to a type of consequent pole machine. In this machine, by reducing the number of magnetic poles and replacing them with iron, the magnetic flux will pass through the iron. This feature has some advantages, such as reducing construction and maintenance costs, reducing leakage flux, increasing linkage flux, and reducing eddy current losses in PMs (due to the flux passing through the iron poles) [18]. Axial flux permanent magnet machines have different types of structures based on the placement of magnets, slots, cores, coils, and multi-stage. In general, these machines can be classified into three categories: single-side, double-side, and multi-stage [7]. Single-side machines consist of one rotor and one stator, the force of attraction between the rotor and the stator in these machines causes unbalance. Multi-stage machines consist of several rotors and stators that are placed in a row, which increases the axial length of the machine. Changing the number of rotors and stators makes it possible to change the torque based on the axial length.

Double-side machines are divided into two categories: Axial flux internal rotor (AFIR) and Axial flux internal stator (AFIS). Both categories are superior in terms of production to single-sided and multi-stage machines. Because, on the one hand, almost no axial magnetic attraction occurs and, on the other hand, they have a simpler structure than multi-stage machines [19-20, 21].

The double rotor structure will be a solution to overcome the axial magnetic attraction force because the net axial force on the rotor is about zero. In addition, it leads to achieving higher power density [22]. In the AFIS structure, the stator is placed in the center, and the permanent magnet rotors on its sides, which results in fewer end windings in the stator. This reduction significantly improves the machine's efficiency [23]. Another name used for machines with internal stator and external rotor combinations is the TORUS structure. Usually, TORUS machines are offered in two types, NN and NS, the main difference of which is the arrangement and sequence of polarity in the poles, the type of winding, and the thickness of the stator yoke [24]. Another way to enhance efficiency is to design a suitable winding for the machine. Using concentrated and non-overlapping coils, in addition to reducing the amount of copper used in the coil head, decreases losses and the overall dimensions of the machine. Moreover, it simplifies the construction of the machine, which subsequently leads to a reduction in production costs [25].

The cogging force produced in a permanent magnet machine due to the interaction between the permanent magnets and the stator teeth causes an undesired vibration and noise. In applications such as robotics there is a need for precise position control and for this purpose force pulsation should be minimized [26]. Several methods have been proposed to reduce cogging torque, such as traditional skewing magnet, selecting appropriate slot opening, pole arc to pole pitch ratio arrangement, and placing flux barrier between 2 slots [25]. Reference [27] has reduced cogging torque value by optimizing the geometrical parameters in surface mounted Permanent Magnet Synchronous Generators (PMSG) and Double-Stator-Single-Rotor (DSSR) topology. Reference [28] discusses the implementation of radially divided magnet shifting to axial flux PM generator with yokeless and segmented armature configuration. The impact of magnet shifting on reducing the cogging torque is also discussed. The proposed design is a permanent magnet divided into 2, 3, 4, and 5 parts and shifted the magnet with a common angle concerning the inner side of the magnet. The results show that a higher number of divided permanent magnets leads to decreased cogging torque, although the higher number of magnet pieces will be challenging in the manufacturing process.

Reference [26] presents a new method for mitigation of the cogging force. It consists of a proper segmentation of the permanent magnets (PMs). By appropriate choosing of the magnet block pitch, the cogging force can be effectively reduced. In Reference [29], the torque ripple of consequent-pole PM machines (CPPMMs) is reduced by injecting order harmonic of the armature current. In the proposed method, based on the machine back-emf spectrum and the current main harmonic, the appropriate order harmonic of the armature current is obtained.

The purpose of this article is to introduce and analyze a sample of a three-phase axial flux permanent magnet generator with a consequent pole structure (CP-PM). The selection of the type of machine is based on several key advantages, including high power density, reduced cogging torque, and low construction cost compared to conventional axial flux generators. The analysis and evaluation of machine performance has been done by 3D finite element analysis in ANSYS Electronic Desktop software. It can be seen that the simple structure, high efficiency, reduced consumption of raw materials, and low manufacturing costs have made the proposed generator an economic model that can be a suitable choice for cars and a suitable replacement for conventional AFPM generators.

## 2-Introducing new structure and modeling

The schematic structure of the proposed permanent axial flux magnet generator with a consequent pole is shown in Figure 1 which consists of a double-side structure with two rotors and one stator. This model has a simple structure to manufacture and also reduces the consumption of magnets which reduces the production costs. A tooth-wound winding is wrapped around the iron teeth of the stator and is placed between the two rotors with an air gap of 1 mm. The used iron for the teeth and the rotor has a relative permeability of 4,000 and a bulk conductivity of 10,300,000 Siemens/m. Sector-shaped magnetic poles made of Nd-Fe-B magnet are placed on the disc-shaped rotor and instead of using magnetic S poles, iron poles (the same type of rotor) are used. The dimensions of the N and S poles are equal. Figure 2 shows the arrangement of machine components from the top view. In this machine, the rotors rotate and the stator is stationary. In Figure 1 the top layer is shown as the front view, if Figure 2 includes the top layer can't show the inside elements like teeth and windings. For this matter, we hide the top layer till can see the all objects. Figure 3 shows the arrangement of machine poles and flux paths in the proposed generator.

Figure 4 shows the arrangement of the coils in the stator. The voltage of each phase of the generator is obtained from the sum of the voltage of two sets of 60-wrapped-up concentrated coils that are connected in series.

In references [3] [4] and [8], due to space limitations, designers have considered eight poles and six concentrated coils for the generator. Figure 5 shows the schematic of the analytical model with a linear structure, in which the sector poles are shown as rectangles. Figure 6 shows the placement of sector poles in a geometric quadrant of the machine, which is made of an N-Iron compound. The radius of the pole and iron is equal to 43 degrees and the distance between them is 2 degrees. The analytical formula of the normal component of the magnetic flux density in the middle of the air gap is [8]:

$$
\begin{aligned}
&B_y\,(x,r) = \hat{B}\cos(ux) = \hat{B}\cos(p\theta)\\
&\tau_p(r) = \frac{\pi r}{p}\\
&u(r) = \frac{\pi}{\tau_p(r)}\\
&\hat{B} = \frac{4}{\tau_p(r)}\frac{B_{rem}}{u(r)\mu_r}\sin\left(0.5u(r)d_m\right)\frac{\sinh(u(r)t_m)}{\sinh\left(u(r)\frac{g}{2}\right)}
\end{aligned}
\qquad (1)
$$

Where, $\tau_p(r)$, $d_m$, $t_m$, $B_{rem}$ , and $\mu_r$ are the pole pitch in different radii, PM width in the circumferential direction, PM thickness, residual flux density, and PM relative permeability, respectively.

Figures 7 and 8 show the coil and teeth of the generator, respectively. The coils are similar to the poles in the form of a sector that is wrapped concentrically around the teeth. To calculate the induced flux and voltage, equation 2 is used:

$$
\begin{aligned}
&V_{coil} = \frac{d\lambda}{dt} \\
&\lambda = \lambda_{\max} \cos(\omega t) \\
&\lambda_{\max} = N \iint B_y \,(r,\theta) r dr d\theta \quad (2) \\
&0 \le r \le 0.5(r_0 + r_i) \\
&0 \le \theta \le 2\pi
\end{aligned}
$$

The formulas are included to give insight into how the air gap flux density obtained by 3D FEM is post-processed to find out the electromagnetic variables such as flux linkages and torque. According to the studies, it is clear that the consequent pole structures are common in radial flux machines and have not been investigated and used in axial flux machines. Therefore, this paper will present a new structure that tries to implement the structure of consequent pole machines in axial flux machines, and from the combination of these two machines, present an optimal and economic model. Since one of the goals of the CP-PM permanent magnet generator is to provide an economic and cost-effective model with similar dimensions, but a higher capacity than the previously built generators, in the modeling process, the dimensions of the generators proposed in references [3] and [8] were considered which is shown in Figure 9. This machine has a double-sided structure with two rotors and one stator. Six circular-shaped coils are arranged in three phases. Eight types of NdFe35 permanent magnets have been used as magnetic poles. The circular-shaped poles are arranged with an N-S structure. The CP-PM generator with the same dimensions was designed. The general specifications of the CP-PM generator are listed in Table No. 1.

## 3-Simulation

### 3.1-Toothless machine

The ANSYS Electronic Desktop software and the finite element analysis method have been selected for simulation. In the first step, the generator was simulated by changing the shape of the poles and coils. The shape changed from a circle to a sector. Assuming the stator to be stationary, the poles mounted on the rotor were rotated at a speed of 1000 rpm by 90 mechanical degrees in the transient mode for 15 milliseconds with time steps of 0.0001 seconds. The voltage and cogging torque variables are considered to be a reference for comparison with the proposed machine. In the second step, by removing the S poles and implementing the consequent pole structure machines, the generator was simulated again with the same conditions as the first step. The results of the variables of voltage, linkage flux, the amount of magnet, and iron consumption are given in table number 2.

Comparing the results of the sector permanent magnet generator and the consequent pole permanent magnet generator shows that with a 50% decrease in the magnet in the CP-PM generator, the flux linkage decreases by only 29.1%, and then the maximum voltage decreases by 28%. It is due to the removal of S poles, which is not unlikely. Also, by reducing the magnet and replacing iron instead of S poles, the amount of iron consumption increased by 39.5%.

Figure 10 shows simultaneously the induction voltage diagram in one phase of the sector generator and the sector consequent pole. The yellow diagram shows the induction voltage of phase A in the sector-PM generator and the blue diagram of phase A of the CP-PM generator. The maximum value of induced voltage in the sector PM generator is equal to 17.5 volts and in the CP-PM generator is equal to 12.6 volts. This 28% reduction in voltage is due to replacing the permanent magnet S pole with an iron pole. As can be seen, the replacement of iron instead of an S pole has only affected the value of the voltage range. The waveform is completely sinusoidal with zero phase difference.

**3.2-Investigation Tooth effect in machine**

By studying and examining the magnet in different states, it is clear that although the magnet plays the main role in permanent magnet machines, there are limitations such as height, width, and magnetic saturation phenomenon. Simulation results in Table number 2 show in the consequent pole machine, the induction voltage is reduced by removing the S poles. One of the ways to increase the induction voltage, use the teeth for coils. The presence of the teeth increases the linkage flux, concentrates and passes the flux through the coil, and reduces the leakage flux. Thus, by adding a tooth to the CP-PM generator, the simulation repeats, and the results are examined again. As can be seen in Figure 11, the presence of the tooth causes the field lines to focus and move towards the coils. With present the tooth, the linkage flux increases, and the leakage flux decreases. The magnetic field strength with adding teeth will be equal to 4.5 ampere per meter on average. Increasing the tooth indeed makes the machine heavier compared to the core-less machine, but this increase in weight can be ignored against the improvement that occurs in the induced voltage.

Figures 12 and 13 show the magnetic flux density in the poles and the back plate of the CP-PM machine, respectively. In Figure 12 upper layer and lower layer poles with the N-Iron structure are shown. It is observed that the flux density in back iron is below 1.8 T which is lower than the field saturation value of the magnetic iron. The variations are not smoothly distributed in some parts of the figures due to the coarse mesh density and numerical errors.

Figures No. 14 and 15 show the induced voltage in the windings of the toothed sector generator and the consequent toothed pole sector. As can be seen, the voltage domain in the consequent pole generator has not changed and is similar to the sector generator. Both generators have similar coils and are turned at 1000 rpm. The three-phase induced voltages are equal to 24.5 volts. They also have a sinusoidal waveform and a 120-degree electrical phase difference with each other. This is even though the amount of magnet used in consequent pole generator has decreased by 50 percent compared to sector generator. In permanent magnet generators, the amount of magnet used has a direct effect on the density of the magnetic field and finally on the amount of induced voltage. In this structure, the effect of a 50% reduction in magnet consumption has been compensated by adding teeth. The addition of the teeth has increased the linkage flux and reduced the leakage flux in the machine. For a better understanding, the A-phase voltage of both generators is shown on a diagram in Figure 16. The blue diagram shows the induction voltage of phase A in the sector-PM generator and the red diagram of phase A of the CP-PM generator. Despite removing S poles in the CP generator and replacing them with iron, the phase difference is equal to zero and the amplitude of voltages are equal.

By examining the linkage flux diagram of the toothed sector generator and the toothed consequent pole sector, it can be seen that with a 50% decrease in the magnet, the linkage flux is reduced by only 17%, but the existence of the tooth prevents the leakage flux and the concentration of the flux in the machine. It also improves the induced voltage. Figure 17 shows the flux linkage diagram of the proposed machine that was obtained from section 2 formulas. The maximum value of the linkage flux is 0.054 Wb for a 10-mm permanent magnet height and 1-mm air gap between permanent magnets and coils on each side, suitable for air-core electric machines.

The machine produced a reluctance torque component. Figures 18 and 19 respectively show the cogging torque of the toothed sector generator and the toothed consequent pole sector. As can be seen, the cogging torque domain in the consequent pole generator has not changed and is similar to the sector generator. The average cogging torque in the sector generator is equal to 127 mNm and in the consequent pole sector generator is equal to 7 mNm. Results show that the proposed structure improves the amount of cogging ripple and average torque. Ripples are due to software numerical errors and can be ignored. However because the simulation was done in three dimensions, it was not possible to reduce the step time. But by reducing the step time, ripples can be eliminated and more accurate results can be obtained.

### 3.3- Under load analysis

To analyze the machine under load, a balanced three-phase variable ohmic load from 1 to 15 ohm was connected to the generator output. This test was performed in the Maxwell circuit section of the Ansys software. In this test, by changing the load value, the output current and load torque were measured in each step. Figures 20 and 21 show the voltage-current and efficiency diagram of the machine at different loads in test mode at a speed of 1000 rpm. It can be seen that the voltage value in the nominal load of 8.5 amps is 22.85 volts and it has only dropped by 2 volts and the efficiency is higher than 92% for a load current of 8.5 A (normal current). The main source of losses in the machine is from stator copper losses. As it was expected, the graphs are linear, because the armature reaction is insignificant. Figure 22, shows the torque diagram under nominal load. These torque curves include components the electromagnetic, reluctance, and cogging torque as well as the torque component due to the interaction of PMs and armature current. As the load increases, the torque value also increases. The average load torque is equal to -2.41 Nm.

### 3.4- Comparing PM Generator & CP-PM Generator

Table No. 3 shows the results of the variables of voltage, linkage flux, magnet, and iron consumption in the toothed sector generator and the toothed consequent pole sector generator. The conditions of both machines are the same and the only change has been made in the arrangement of the poles of the machine. By reducing the magnet by 50%, the linkage flux will decrease by 17%. However, the iron consumption in the poles and teeth in the consequent pole machine increased by 37.5% compared to the sector pole machine. Despite these changes and the reduction in magnet consumption, the induced voltage is maintained in the desired range, and in addition, the cogging torque is optimized. Also, the phase difference between the induced voltages by the coils is equal to 120 degrees.

## 4-Conclusion

Previously, using the structure of a consequent pole has been common in radial flux machines and has not been used in axial flux machines. Therefore, according to the advantages of consequent pole machines, this article presented a model of an axial flux generator with consequent poles. In permanent magnet machines, the magnet plays an essential role, since the cost of producing this type of magnet is very high compared to iron, by presenting this new structure, while significantly reducing the consumption of magnets, and then reducing production costs. The variable induction voltage in the coils has not changed compared to the permanent magnet sector generator, which has all its poles made of magnets and is equal to 24.5 volts in both machines. Also, the effect of the consequent pole structure in reducing the torque is evident, so that the cogging torque ripple of the consequent pole generator is much less than that of the sector generator.

By comparing the sector pole generator and the consequent pole generator, it can be seen that in the structure of the consequent pole, the amount of magnet consumption has decreased by 50% and the iron consumption has increased by 37.5%. Considering the higher price of a permanent magnet (about 10 times) compared to the price of iron, using this design significantly saves production costs. According to the investigations, the optimal structure is the simultaneous use of consequent poles and a toothed stator.

This topology has several advantages such as reducing the consumption of rare-earth permanent magnets, reducing environmental hazards, lowering material and manufacturing costs with better performance, simple and robust structure, simple rotor construction, simple winding, very low cogging torque, and favorable electrical characteristics. It also has lower losses and higher efficiency which make us achieve an efficient and economical machine. The disadvantage of this machine is the slightly higher weight than the coreless machine. That is due to using an iron tooth in the proposed construction.

## 5-Reference


[1] Rahim, NA., Hew, WP., and Mahmoudi, A. “Axial flux permanent-magnet brushless dc traction motor for direct drive of electric vehicle,” Int. Rev. Elect.l Eng.,Vol. 6, No. 2, 760-769, April (2011).

[2] Izumiya, K., Tsunata, R., Takemoto, M., et al. "Axial-Flux Machine Using Ferrite PM and Round Wire Competitive to Radial-Flux Machine Using Nd-Fe-B PM for HEV Traction," 2022 International Conference on Electrical Machines (ICEM), pp. 192-198, doi: 10.1109/ICEM51905.2022.9910903, Valencia, Spain, (2022).

[3] Javadi, S., and Mirsali , M. " Design and Analysis of 42-V Coreless Axial-Flux Permanent-Magnet Generators for Automotive Applications ", IEEE Transactions on Magnetics, Volume: 46, Issue: 4, pp: 1015 – 1023, ISI, Apr (2010).

[4] Javadi, S., and Mirsali , M. “A Coreless Axial-Flux Permanent-Magnet Generator for Automotive Applications”, IEEE Transactions on Magnetics, Volume: 44, Issue: 12, pp: 4591- 4598, Dec. ISI (2008).

[5] Taqavi, O., Abdollahi, SE., and Aslani, B. "Investigations of Magnet Shape Impacts on Coreless Axial-Flux PM Machine Performances," 2021 12th Power Electronics, Drive Systems, and Technologies Conference (PEDSTC), pp. 1-5, doi: 10.1109/PEDSTC52094.2021.9405833, Tabriz, Iran (2021).

[6] Zhao, J., Quan, X., Sun, X., et al. "Design of a Novel Axial Flux Rotor Consequent-Pole Permanent Magnet Machine," in IEEE Transactions on Applied Superconductivity, vol. 30, no. 4, pp. 1-6, Art no. 5205506, doi: 10.1109/TASC.2020.2986743, June (2020).

[7] Kahourzade, S., Mahmoudi, A., Ping, HW., et al. "A Comprehensive Review of Axial-Flux Permanent-Magnet Machines," in Canadian Journal of Electrical and Computer Engineering, vol. 37, no. 1, pp. 19-33, doi: 10.1109/CJECE.2014.2309322, winter (2014).

[8] Patterson, DJ., Colton, JL., Mularcik, B., et al. "A comparison of radial and axial flux structures in electrical machines," 2009 IEEE International Electric Machines and Drives Conference, pp. 1029-1035, doi: 10.1109/IEMDC.2009.5075331, Miami, FL, USA (2009).

[9] Chimento, F., and Raciti, A. "A low-speed axial-flux PM generator for wind power systems," *2004 IEEE International Symposium on Industrial Electronics*, pp. 1479-1484 vol. 2, doi: 10.1109/ISIE.2004.1572032, Ajaccio, France (2004).

[10] Nishanth, F., Van Verdeghem, J., and Severson, EL. "A Review of Axial Flux Permanent Magnet Machine Technology," in IEEE Transactions on Industry Applications, vol. 59, no. 4, pp. 3920-3933, doi: 10.1109/TIA.2023.3258933, July-Aug (2023).

[11] Taghipour Boroujeni, S., Emami, SP., Takorabet, N., et al. "Analytical investigation of the armature current influence on the torque and radial force in eccentric consequent-pole PM machines". IET Electric Power Applications, Volume15, Issue4, Pages 441-452, https://doi.org/ 10.1049/elp2.12037, April (2021).

[12] Asgari, S., Saed, N., and Muetze, A. "Low-Cost Axial Flux PCB Motor with Ferrite Core and Ferrite Magnet Topology for Fan Applications," 2023 IEEE International Electric Machines & Drives Conference (IEMDC), pp. 1-5, doi: 10.1109/IEMDC55163.2023.1023889, San Francisco, CA, USA (2023).

[13] Kobler, R., Andessner, D., Weidenholzer, G., et al. "Development of a compact and low cost axial flux machine using soft magnetic composite and hard ferrite," 2015 IEEE 11th International Conference on Power Electronics and Drive Systems, pp. 810-815, doi: 10.1109/PEDS.2015.7203383, , Sydney, NSW, Australia (2015).

[14] Izumiya, K., Tsunata, R., Takemoto, M., et al. "Axial-Flux Machine Using Ferrite PM and Round Wire Competitive to Radial-Flux Machine Using Nd-Fe-B PM for HEV Traction," 2022 International Conference on Electrical Machines (ICEM), pp. 192-198, doi: 10.1109/ICEM51905.2022.9910903, Valencia, Spain (2022).

[15] Chulaee, Y., Lewis, D., Vatani, M., et al. "Torque and Power Capabilities of Coreless Axial Flux Machines with Surface PMs and Halbach Array Rotors," 2023 IEEE International Electric Machines & Drives Conference (IEMDC), pp. 1-6, doi: 10.1109/IEMDC55163.2023.10239021, San Francisco, CA, USA (2023).

[16] Lu, Y., Kai, Y., Songjun, S., et al. "Axial Flux Permanent Magnet Electrical Machine with High Torque Density: Research on the Influence of Combined-Halbach Array on YASA Machine," 2023 IEEE International Magnetic Conference - Short Papers (INTERMAG Short Papers), pp. 1-2, doi: 10.1109/INTERMAGShortPapers58606.2023.10228726, Sendai, Japan (2023).

[17] Chung, SU., Kim, JW., Chun, YD., et al. "Fractional Slot Concentrated Winding PMSM With Consequent Pole Rotor for a Low-Speed Direct Drive: Reduction of Rare Earth Permanent Magnet" in IEEE Transactions on Energy Conversion, vol. 30, no. 1, pp. 103-109, doi: 10.1109/TEC.2014.2352365, March (2015).

[18] Ghaffari, A., Rahideh, A., Moayed-Jahromi, H., et al. "2-D Analytical Model for Outer-Rotor Consequent-Pole Brushless PM Machines," in IEEE Transactions on Energy Conversion, vol. 34, no. 4, pp. 2226-2234, doi: 10.1109/TEC.2019.2941935, Dec (2019).

[19] Lehr, M., Woog, D., and Binder, A. "Design, construction and measurements of a permanent magnet axial flux machine," 2016 XXII International Conference on Electrical Machines (ICEM), pp. 1604-1610, doi: 10.1109/ICELMACH.2016.7732738, Lausanne, Switzerland (2016)

[20] Aydin, M., Huang, S., and Lipo, TA. "Torque quality and comparison of internal and external rotor axial flux surface-magnet disc machines," in IEEE Transactions on Industrial Electronics, vol. 53, no. 3, pp. 822-830, doi: 10.1109/TIE.2006.874268, June (2006).

[21] Lehr, M., Reis, K., and Binder, A. "Comparison of axial flux and radial flux machines for the use in wheel hub drives", e+i Elektrotechnik und Informationstechnik, Volume 132, pages 25–32, https://doi.org/10.1007/s00502-014-0272-3, (2015).

[22] Nobahari, A., Darabi, A., and Hassannia, A. "Axial flux induction motor, design and evaluation of steady state modeling using equivalent circuit," 2017 8th Power Electronics, Drive Systems & Technologies Conference (PEDSTC), pp. 353-358, doi: 10.1109/PEDSTC.2017.7910351, Mashhad, Iran (2017).

[23] Babu, VR., Soni, MP., and Manjeera, C. "Modeling of axial flux induction machine with sinusoidal winding ribution," 2012 Annual IEEE India Conference (INDICON), pp. 481-486, doi: 10.1109/INDCON.2012.6420666, Kochi, India (2012).

[24] Huang, S., Aydin, M., and Lipo, TA. "TORUS concept machines: pre-prototyping design assessment for two major topologies," Conference Record of the IEEE Industry Applications Conference. 36th IAS Annual Meeting (Cat. No.01CH37248), 2001, pp. 1619-1625 vol.3, doi: 10.1109/IAS.2001.955751, Chicago, IL, USA (2001).

[25] Kobler, R., Andessner, D., Weidenholzer, G., et al. "Development of a compact and low cost axial flux machine using soft magnetic composite and hard ferrite," 2015 IEEE 11th International Conference on Power Electronics and Drive Systems, pp. 810-815, doi, Sydney, NSW, Australia (2015).

[26] Shabani, MA., Milimonfared, J., and Taghipour, S. "Cogging force mitigation of tubular permanent magnet machines with magnet dividing," *2007 International Conference on Electrical Machines and Systems (ICEMS)*, Seoul, pp. 810-814, doi: 10.1109/ICEMS12746.2007.4412196, Korea (South) (2007).

[27] Gul, W., Gao, Q., Walker, A., et al. "Mitigation of Cogging Torque in a Double-Stator Single-Rotor PMSG for Direct Drive Offshore Wind Turbines," 2023 IEEE International Electric Machines & Drives Conference (IEMDC), pp. 1-6, doi: 10.1109/IEMDC55163.2023.10238922, San Francisco, CA, USA (2023).

[28] Imanuddin, N., Furqani, J., and Rizqiawan, A. "Effects of Radial Divided Magnet Shifting on Cogging Torque of Axial Flux Permanent Magnet Generator for Small Scale Wind Turbine," 2023 4th International Conference on High Voltage Engineering and Power Systems (ICHVEPS), pp. 555-560, doi: 10.1109/ICHVEPS58902.2023.10257501, Denpasar Bali, Indonesia (2023).

[29] Taghipour Boroujeni, S., Emami, SP., Takorabet, N., et al. "Torque ripple minimization in Consequent-Pole PM Machines using harmonic current injection" Scientia Iranica, Volume & Issue: Articles in Press Number of Articles: 409, pp.1-7, -. doi: 10.24200/sci.2022.60312.6725, (2022).

## Figure:



**Table:**

**Mahmoud Marousi Noushabadi** was born in Kashan, Iran, on 1989. He received a B.Sc. degree in electrical engineering from Technical and Vocational University, Kermanshah, Iran, in 2012 and an M.Sc. degree in electrical power engineering from Islamic Azad University, Kashan, Iran in 2016. He is currently a Ph.D. student in Electrical Power Engineering at Islamic Azad University, Kashan, Iran. His special fields of interest include designing, analyzing, and optimizing electric machines and hybrid vehicles.

**Saeid Javadi** was born in Aran and Bidgol, Iran, on March 21, 1969. He received the B.Sc. degree in communication engineering and the M.Sc. and Ph.D. degrees in electrical power engineering from Amirkabir University of Technology, Tehran, Iran, in 1992, 1999 and 2010, respectively. He is currently an Assistant Professor in the Department of Electrical and Computer Engineering, Kashan Branch, Islamic Azad University, Kashan, Iran. His special fields of interest include the design, analysis and optimization of electric machines and hybrid vehicles.

**Samad Taghipour Boroujeni** received the B.Sc., M.Sc., and Ph.D. degrees in electrical engineering from the Department of Electrical Engineering, Amirkabir University (Tehran Polytechnic), Tehran, Iran, in 2003, 2005, and 2009, respectively. In 2008, he was a Visiting Scholar with the Electrical Engineering Department, Padova University, Padova, Italy. In 2009, he joined the Department of Engineering, Shahrekord University, Shahrekord, Iran, as an Assistant Professor, where he was serving as an Associate Professor from 2016 to 2020. He had a postdoctoral carrier in 2018-2020 in Lorrain University, Nancy, France in GREEN Lab. He has been a Full Prof. since 2020 at Shahrekord University. His research interests include modeling, design, analysis, optimization, and control of electrical machines, especially variable-speed generators.

**List of Figure:**

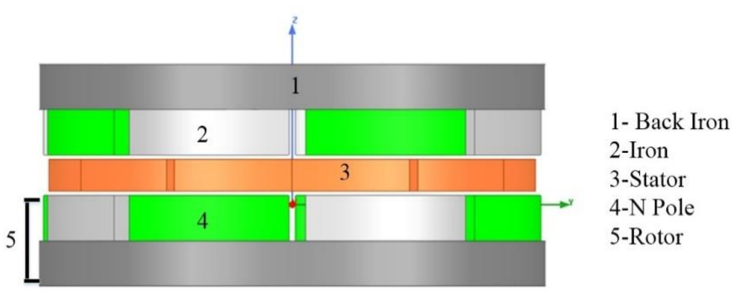


**Fig 1.** Structure of the proposed model

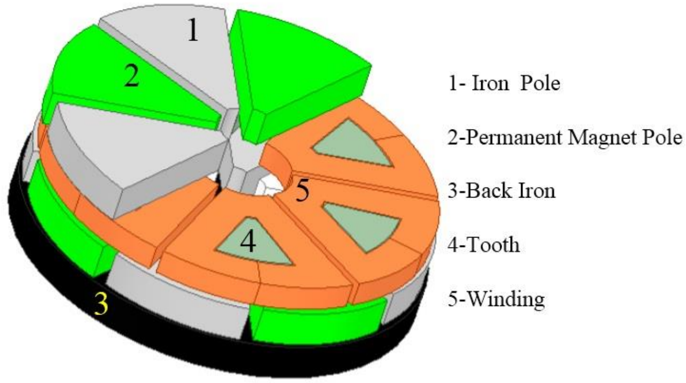


**Fig 2.** Top view of the proposed model

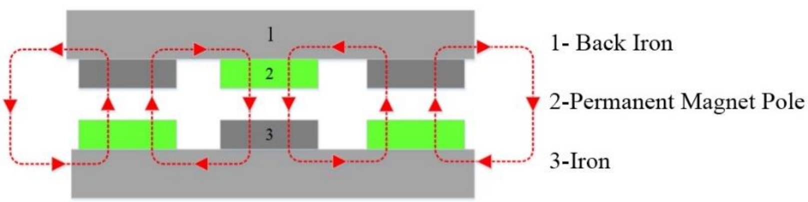


**Fig 3.** Magnetic flux path

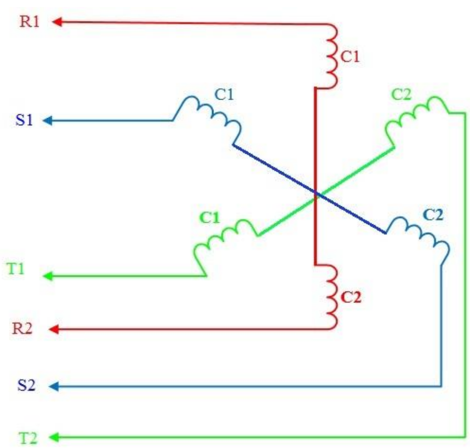


**Fig 4.** Coils arrangement

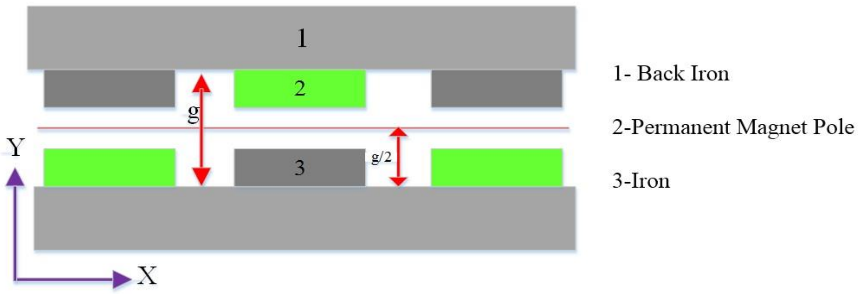


**Fig 5.** Schematic of analytical model with linear structure

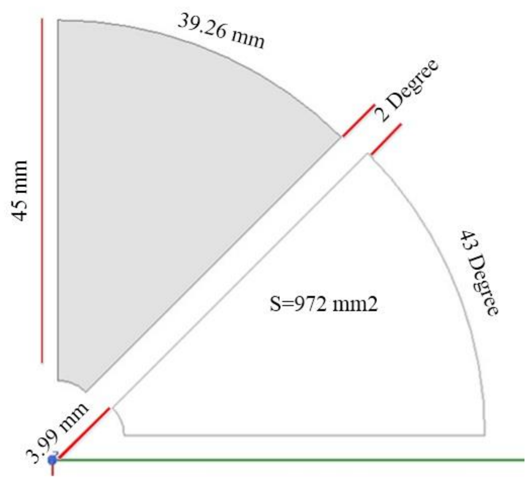


**Fig 6.** The dimensions of the sector poles

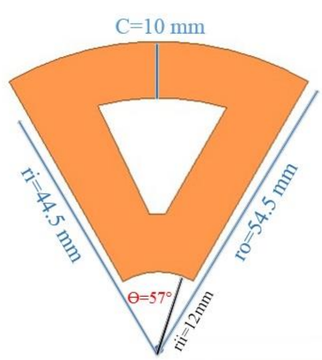


**Fig 7.** Stator coil

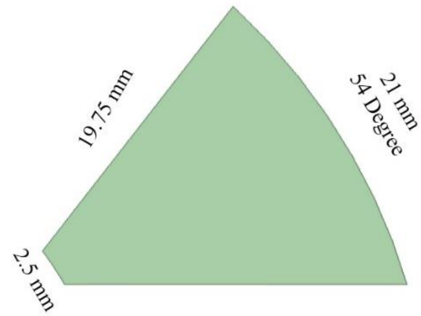


**Fig 8.** Stator tooth

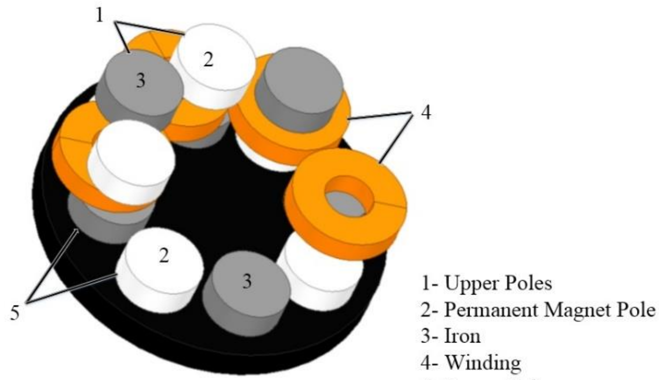


**Fig 9.** Machine structure with circular poles and windings

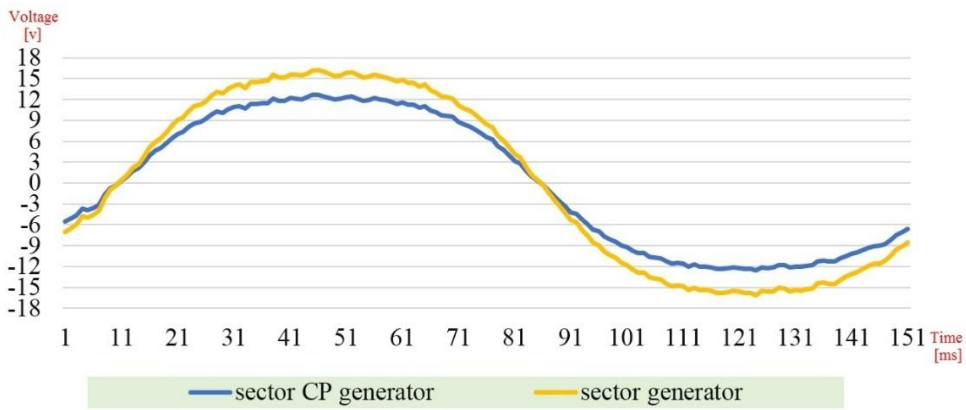


**Fig 10.** Induced voltage of sector generator and the sector consequent pole

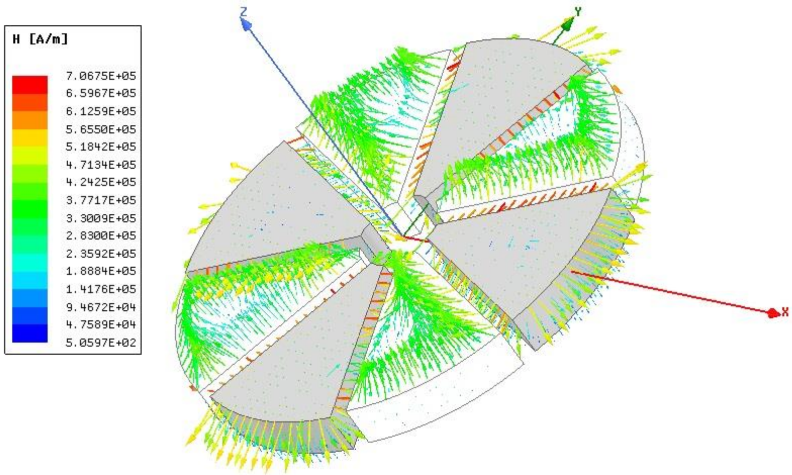


**Fig 11.** Path and concentration of the flux towards the teeth

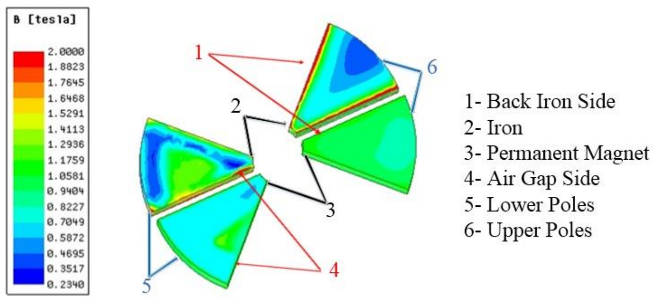


**Fig 12.** Magnetic flux density in CP-PM generator poles

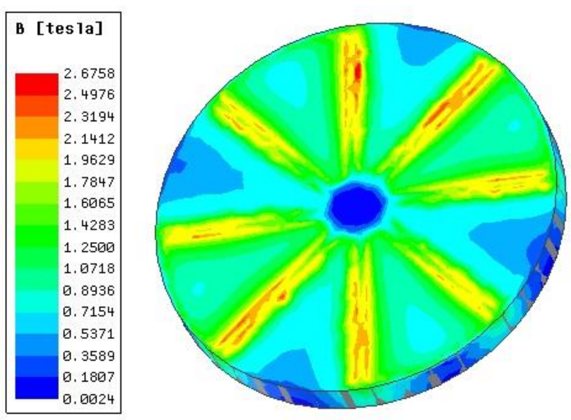


**Fig 13.** Flux density in the back plate the CP-PM generator poles

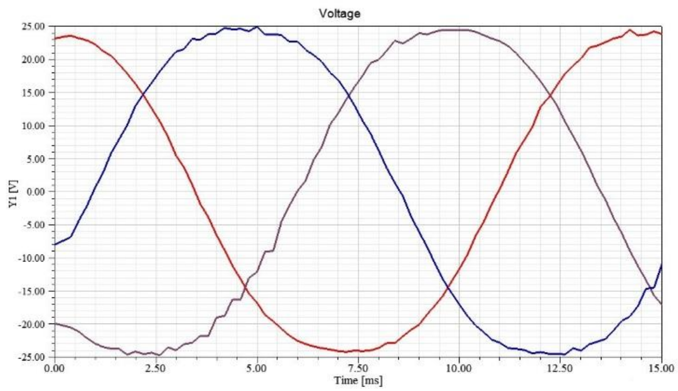


| Curve Info | max | Pk2pk |
|---|---|---|
| --- Induced Voltage (R) | 24.42 | 48.58 |
| --- Induced Voltage (S) | 24.40 | 49.09 |
| --- Induced Voltage (T) | 24.88 | 49.43 |

**Fig 14.** Induced voltage of toothed sector generator

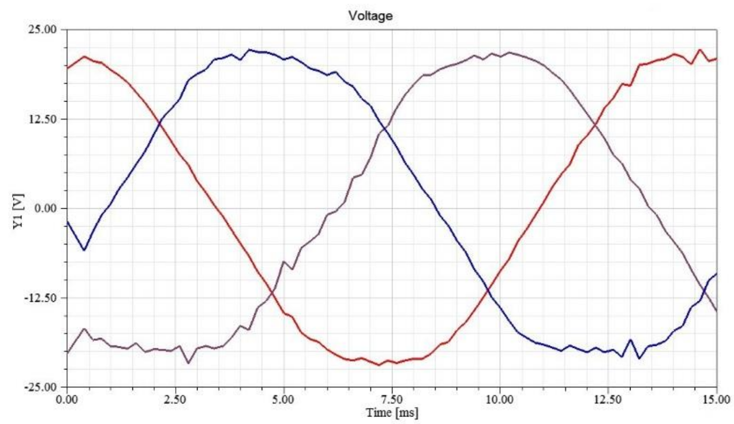


| Curve Info | max | Pk2pk |
|---|---|---|
| --- Induced Voltage (R) | 23.73 | 45.38 |
| --- Induced Voltage (S) | 24.13 | 45.13 |
| --- Induced Voltage (T) | 24.21 | 46.08 |

**Fig 15.** Induced voltage of a toothed consequent pole sector generator

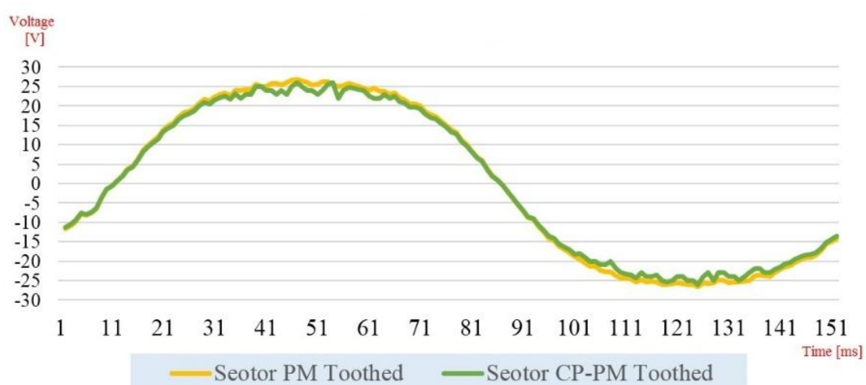


**Fig 16.** Induced voltage of toothed sector generator and toothed consequent pole sector generator

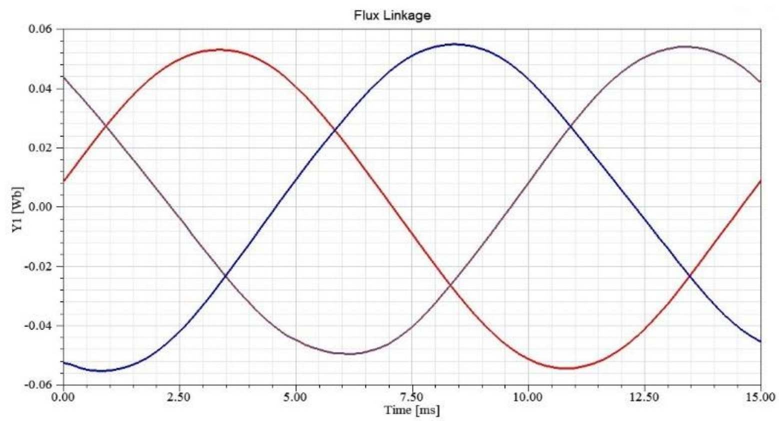


| Curve Info | max |
| --- | --- |
| --- Flux Linkage (R) | 0.0529 |
| --- Flux Linkage (S) | 0.0538 |
| --- Flux Linkage (T) | 0.0547 |

**Fig 17.** Linkage flux of CP-PM generator

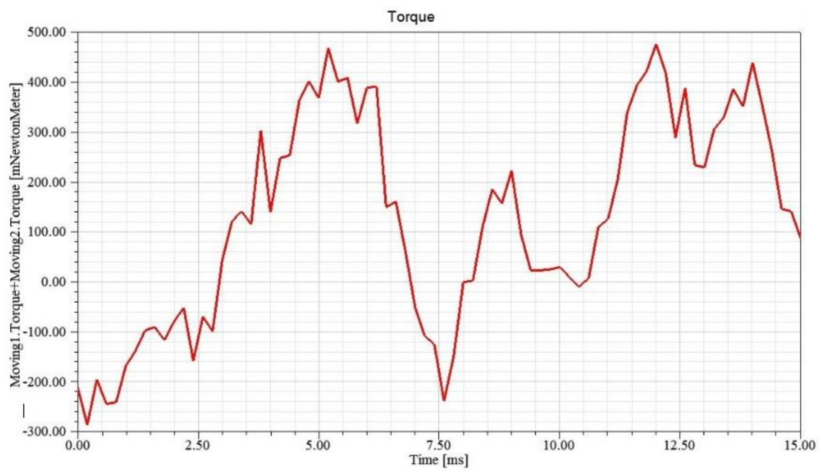


| Curve Info | Ave |
| --- | --- |
| --- Torque | 127.12 |

**Fig 18.** Cogging torque in toothed sector generator

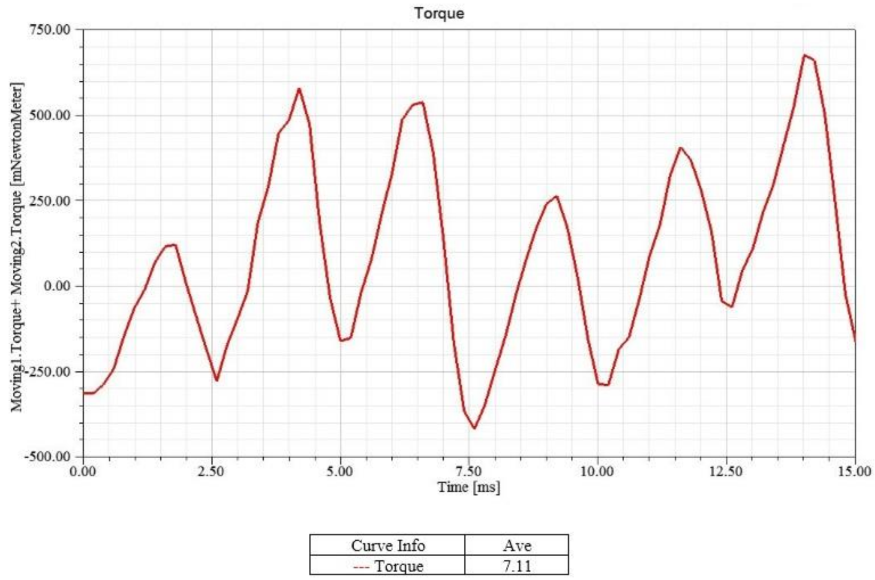


**Fig 19.** Cogging torque in toothed consequent pole sector generator

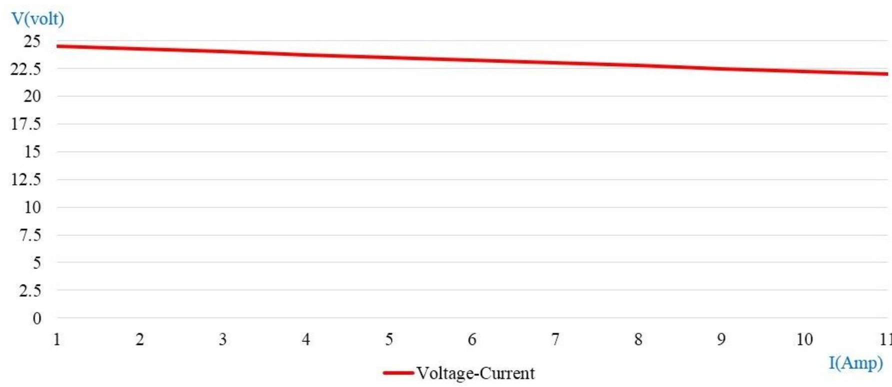


**Fig 20.** Machine Voltage - Current diagram at different loads

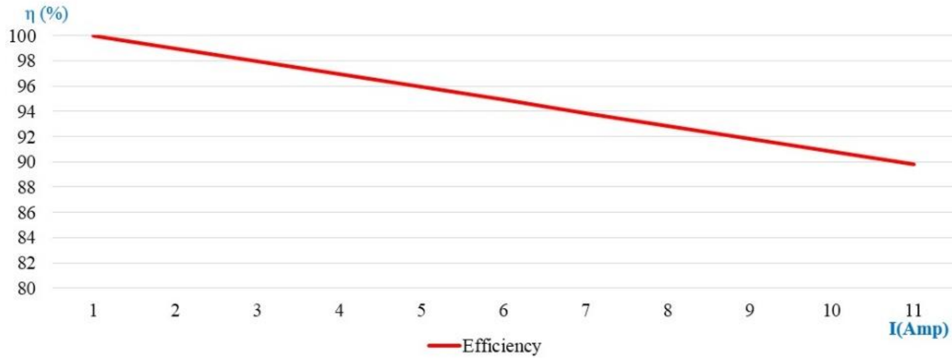


**Fig 21.** Efficiency diagram at different loads

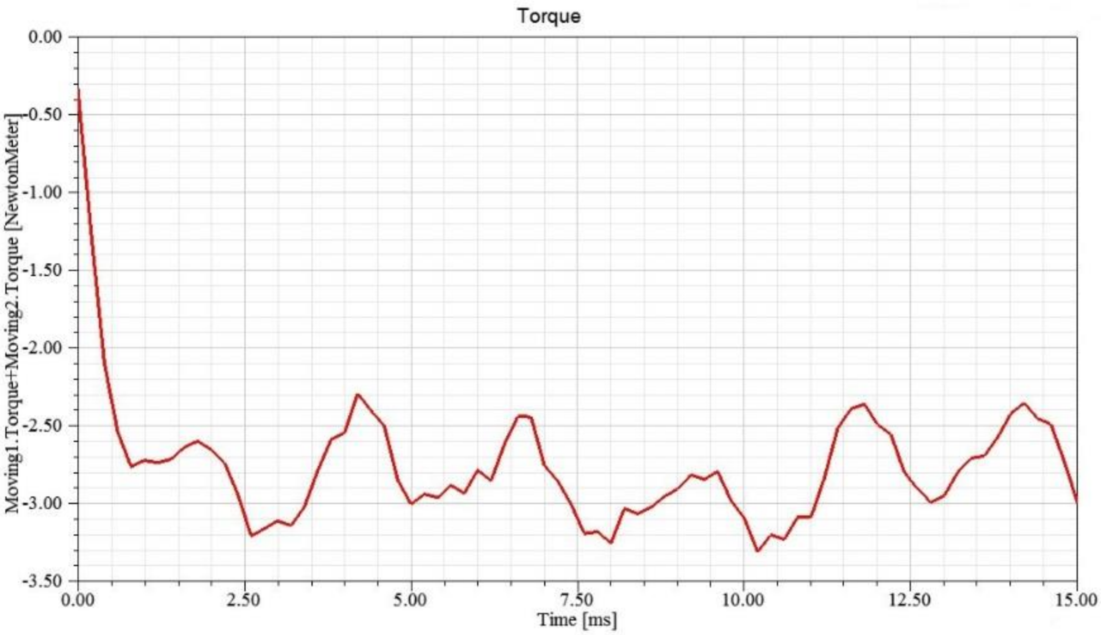


| Curve Info | Ave |
|---|---|
| --- Torque | -2.415 |

**Fig 22.** Torque diagram under nominal load

**List of table:**

**Table 1.** Characteristics of consequent pole permanent magnet generator

| **Parameter** | **Values** |
|---|---|
| Number Of Phases | 3 |
| Number Of Coils | 6 |
| $N_{Coil}$ | 60 |
| $N_{S\ Phase}$ | 120 |
| Wire Diameter | 0.75 (mm) |
| Number Of Poles (NdFe35) | 8 |
| $B_{rem}$ Residual Flux Density Of PM | 1.2 (T) |
| Outer Radial Length Of PM | 45 (mm) |
| Inner Radial Length Of PM | 4 (mm) |
| Permanent Magnet Arc Angel | 43° |
| Distance Between Poles | 2° |
| Pole Thickness | 10 (mm) |
| Thickness Of Back Iron | 10 (mm) |
| Outer Radius Of Back Iron Disc | 55 (mm) |
| Axial Length Of Generator | 52 (mm) |
| Air Gap | 1 (mm) |
| Outer Radial Length Of Coil (ro) | 54.5 (mm) |
| Inner Radial Length Of Coil-1 (ri) | 44.5 (mm) |
| Inner Radial Length Of Coil-2 (rii) | 12 (mm) |
| Coil Width | 10 (mm) |
| Coil Height | 10 (mm) |
| Coil Arc Angele | 57° |
| Tooth Length | 19.75 (mm) |
| Tooth Width | 2.5 (mm) |
| Tooth Arc Angele | 54° |

| | |
|---|---|
| Speed | 1000 (rpm) |

**Table 2.** The results of the analysis of the sector generator and consequent pole generator

| **Machine Type** | **Sector PM Generator** | **Sector CP-PM Generator** | **Sector PM Percentage changes relative to Sector CP-PM [%]** |
|---|---|---|---|
| **Induced Voltage (V)** | 17.5 | 12.6 | -28 |
| **Linkage Flux (Wb)** | 0.0466 | 0.033 | -29.1845494 |
| **Magnet Used (mm3)** | 155488 | 77744 | -50 |
| **Iron Used (mm3)** | 197040 | 274784 | 39.45594803 |

**Table 3.** PM & CP-PM Generator analysis results

| **Machine Type** | **PM Generator** | **CP-PM Generator** | **CP-PM percentage changes relative to PM [%]** |
|---|---|---|---|
| **Induced Voltage (V)** | 24.5 | 24.5 | 0 |
| **Linkage Flux (Wb)** | 0.0615 | 0.051 | -17.0731707 |
| **Magnet Used (mm3)** | 155488 | 77752 | -49.9948549 |
| **Iron Used (mm3)** | 206640 | 284392 | 37.62679055 |